J. Am. Chem. Soc. **1982**, *104*, 74-82

Electrostatic Binding of Electroactive and Nonelectroactive Anions in a Surface-Confined, Electroactive Polymer: Selectivity of Binding Measured by Auger Spectroscopy and Cyclic Voltammetry

James A. Bruce and Mark S. Wrighton*

Contribution from the Department of Chemistry, Massachusetts Institute of Technology, Cambridge, Massachusetts 02139. *Received June 1, 1981*

Abstract: Electrodes can be functionalized with {*N*,*N*′-bis(3-(trimethoxysilyl)propyl)-4,4′-bipyridinium} dibromide (I), yielding a surface-confined, electroactive polymer, $(PQ^{2+}\cdot 2Br^-)_n$. The anions are labile and can be replaced readily by a number of anions. By a combination of Auger and electrochemical techniques we have studied the incorporation of the anions *p*-toluenesulfonate, Cl^-, Br^-, I^-, ClO_4^-, SCN^-, SO_4^{2-}, $Fe(CN)_6^{4-}$, $Ru(CN)_6^{4-}$, $Co(CN)_6^{3-}$, $Mo(CN)_8^{4-}$, $IrCl_6^{2-}$, and $PtCl_6^{2-}$ into $(PQ^{2+})_n$. Generally, the transition metal complex anions are more firmly bound and less labile than the other anions. The ordering of monoanions is *p*-toluenesulfonate $\simeq Cl^- < Br^- \simeq ClO_4^- \simeq SCN^- < I^-$. The SO_4^{2-} anion competes well with ClO_4^- and not as well with I^-. For the monoanions and SO_4^{2-} the selectivity for binding spans a range of approximately an order of magnitude. For example, a solution having 0.09 M Cl^- and 0.01 M I^- has ~50% I^- and ~50% Cl^- in the $(PQ^{2+})_n$. The selectivity for binding $IrCl_6^{2-}$, the most weakly bound transition metal complex, is considerable. For example, a solution having 0.1 M SO_4^{2-} and 5×10^{-5} M $IrCl_6^{2-}$ gives >50% $IrCl_6^{2-}$ in the $(PQ^{2+})_n$ when analyzed by auger spectroscopy after removal from the solution followed by washing. The complexes $Mo(CN)_8^{4-}$, $Fe(CN)_6^{4-}$, $Ru(CN)_6^{4-}$, and $IrCl_6^{2-}$ exhibit chemically reversible redox reaction when bound to the polymer, as determined by cyclic voltammetry. Such electroactive anions can be bound in the $(PQ^{2+})_n$ polymer for prolonged periods (>1 h) in the presence of 0.1 M KCl. Cyclic voltammetry of electrodes having variable amounts of $IrCl_6^{3-}$, $(PQ^{2+}\cdot{}^2/_3xIrCl_6^{3-} + (1-x)SO_4^{2-})_n$ (x = 0–1), correlates well with intensity of Auger signals characteristic of $IrCl_6^{3-}$ relative to those for $(PQ^{2+})_n$, providing confidence in our use of Auger to order the binding of nonelectroactive anions. Electrochemistry allows an ordering of $IrCl_6^{2-} < Fe(CN)_6^{4-} \approx Ru(CN)_6^{4-} < Mo(CN)_8^{4-}$ for the electroactive ions. The effect of $Co(CN)_6^{3-}$ on the electrochemistry of $Fe(CN)_6^{4-}$ and $Mo(CN)_8^{4-}$ places $Co(CN)_6^{3-}$ near $Ru(CN)_6^{4-}$ in this ordering.

Electrodes derivatized with electroactive polymers or with charged, nonelectroactive polymers can be significantly influenced by the nature of the electrolyte and other ions present in a solution contacted by the derivatized electrode. It has been shown that charged, nonelectroactive polymers can persistently bind significant quantities of charged, electroactive species such as $Fe(CN)_6^{4-}$ by surface polyvinylpyridinium[1-3] or $Ru(bpy)_3^{2+}$ by Nafion.[4] These examples illustrate how electrostatic binding may be exploited for analysis, preparation of a variety of modified electrodes, and study of electrocatalysis. Electroactive polymers are charged in at least one of their accessible redox states, and both selectivity of counterion binding and the movement of ions in and out of the surface polymer associated with change of redox state may affect electrochemical behavior.[5-7] Electrodes coated with electroactive polymers may have a number of uses,[8] including desalting of H_2O,[9] depending on the behavior of solution ions.

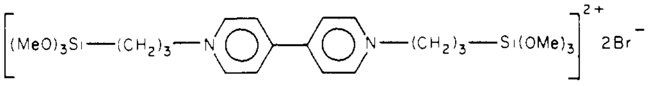

1

Recent work in this laboratory[10,11] has involved the use of reagent I to functionalize photocathode surfaces yielding a surface-confined electroactive polymer, $(PQ^2\cdot 2Br^-)_n$. The ability to observe essentially reversible redox chemistry for the $(PQ^{2+})_n$ in aq. KBr suggests good mobility for the anions, eq 1a, and/or the

$$\text{surface-}(PQ^{2+}\cdot 2Br^-)_n + ne^- \xrightleftharpoons{-0.5\text{ V vs. SCE}} \text{surface-}(PQ^{+\cdot}\cdot Br^-)_n + nBr^- \quad (1a)$$

cations, eq 1b. We exploited the lability of the anions to in-

$$\text{surface-}(PQ^{2+}\cdot 2Br^-)_n + ne^- + nK^+ \xrightleftharpoons{-0.5\text{ V vs. SCE}} \text{surface-}(PQ^{+\cdot}\cdot K^+\cdot 2Br^-)_n \quad (1b)$$

corporate Pt(0) in the polymer as a hydrogen evolution catalyst[11] (eq 2 and 3). In this article we put our preliminary results for

$$\text{surface-}(PQ^{2+}\cdot 2Br^-)_n + nK_2PtCl_6 \rightarrow \text{surface-}(PQ^{2+}\cdot PtCl_6^{2-})_n + 2nKBr \quad (2)$$

$$\text{surface-}(PQ^{2+}\cdot PtCl_6^{2-})_n \xrightarrow[KBr]{\text{reduce}} \text{surface-}(PQ^{2+}\cdot 2Br^-/Pt(0))_n + 6nCl^- \quad (3)$$

$PtCl_6^{2-}$ incorporation on a quantitative footing and amplify our studies of ion exchange involving both electroactive and nonelectroactive anions. Of particular importance is the establishment of Auger spectroscopy as a good tool for determining the presence, and relative amount, of ions such as Cl^-, Br^-, etc., that are difficult to determine by other techniques. It has been claimed that X-ray photoelectron spectroscopy is a useful technique to detect such anions on modified electrode surfaces.[12] The electrodes that have been studied are Pt and p-type Si,[11] but the results should be

---

[1] Oyama, N.; Anson, F. C. *J. Electrochem. Soc.* **1980**, *127*, 247; *Anal. Chem.* **1980**, *52*, 1192.

[2] Shigehara, K.; Oyama, N.; Anson, F. C. *Inorg. Chem.* **1981**, *20*, 518.

[3] Oyama, N.; Sato, K.; Matsuda, H. *J. Electroanal. Chem.* **1980**, *115*, 149.

[4] Rubinstein, I.; Bard, A. J. *J. Am. Chem. Soc.* **1980**, *102*, 6641.

[5] (a) Schroeder, A. H.; Kaufman, F. B. *J. Electroanal. Chem.* **1980**, *113*, 209. (b) Schroeder, A. H.; Kaufman, F. B.; Patel, V.; Engler, E. M. *Ibid.* **1980**, *113*, 193. (c) Kaufman, F. B.; Schroeder, A. H.; Engler, E. M.; Kramer, S. R.; Chambers, J. Q. *J. Am. Chem. Soc.* **1980**, *102*, 483.

[6] Oyama, N.; Anson, F. C. *J. Am. Chem. Soc.* **1979**, *101*, 739, 3450; *J. Electrochem. Soc.* **1980**, *127*, 640.

[7] Wrighton, M. S.; Palazzotto, M. C.; Bocarsly, A. B.; Bolts, J. M.; Fischer, A. B.; Nadjo, L. *J. Am. Chem. Soc.* **1978**, *100*, 7264.

[8] Murray, R. W. *Acc. Chem. Res.* **1980**, *13*, 135.

[9] Factor, A.; Rouse, T. O. *J. Electrochem. Soc.* **1980**, *127*, 1313.

[10] Bookbinder, D. C.; Wrighton, M. S. *J. Am. Chem. Soc.* **1980**, *102*, 5123.

[11] (a) Bookbinder, D. C.; Bruce, J. A.; Dominey, R. N.; Lewis, N. S.; Wrighton, M. S. *Proc. Natl. Acad. Sci. U.S.A.* **1980**, *77*, 6280. (b) Dominey, R. N.; Lewis, N. S.; Bruce, J. A.; Bookbinder, D. C.; Wrighton, M. S. *J. Am. Chem. Soc.*, in press.

[12] Moses, P. R.; Murray, R. W. *J. Am. Chem. Soc.* **1976**, *98*, 7435.

0002-7863/82/1504-0074\$01.25/0

directly extendable to any other surface modified with I.

Experimental Section

Electrodes and Derivatization. Single-crystal p-Si wafers (0.35 mm thick, (111) face exposed), doped with B (resistivity, 3-7 ohm cm), were obtained from Monsanto Co., Electronics Division (Palo Alto, CA). Ohmic contact to the back of the electrode was made by vapor deposition of Al then sintering at 723 K under N_2 for 5 min. Electrodes were mounted as previously described.[10,11] Typical electrode areas ranged from 10 to 25 mm^2.

Synthesis of I has been previously described.[10,11] For derivatization of Si, the Si electrodes are first etched in concentrated HF at 298 K for 60 s then rinsed in distilled H_2O and dipped in 10 M NaOH at 298 K for 60 s. The electrode is then rinsed again in distilled H_2O, followed by acetone and air-dried. The electrodes are then immersed in a 1-5 mM solution of I in CH_3CN under N_2 and left for 3-48 h at 298 K. After removal from solution, the electrodes are rinsed with CH_3CN and stored under Ar. Pt foil electrodes are electrochemically pretreated as previously described.[13] Pt electrodes were then derivatized with I either by immersion into 1-5 mM solutions of I in CH_3CN, or by potentiostatting the electrodes at -0.72 V vs. SCE in aqueous 0.1 M K_2HPO_4, 0.2 M KCl, ~3 mM I. Coverage of electroactive $(PQ^{2+})_n$ was determined by integration of the cyclic voltammetric wave associated with $(PQ^{2+})_n \rightleftarrows (PQ^{+\cdot})_n$.

Electrochemical Equipment. Cyclic voltammograms were obtained using a PAR Model 173 potentiostat, a Model 175 programmer, and a Houston Instruments 2000 XY recorder. All experiments were performed in a single compartment Pyrex cell equipped with a saturated calomel reference electrode (SCE), a Pt wire counterelectrode, and a Pt or p-Si working electrode. The solution contained 0.1 M supporting electrolyte. Reagent grade chemicals and distilled, deionized H_2O were used. Studies involving electrodes derivatized with I were carried out under Ar. p-Si electrodes were illuminated with a beam expanded 632.8-nm He-Ne laser (Aerotech or Coherent Radiation) providing up to ~50 mW/cm^2.

Ion Exchange into $(PQ^{2+})_n$ Polymer. Replacing the Br^- in $(PQ^{2+}\cdot 2Br^-)_n$ by another anion was accomplished by placing the electrode into an aqueous solution of the appropriate ions. The electrode was then left to equilibrate at 298 K for a period of time long enough to ensure that equilibrium was established. The electrode was then well-rinsed with distilled, deionized H_2O to remove any excess electrolyte.

Auger Spectroscopy. Auger spectra were obtained on a Physical Electronics Model 590A scanning Auger spectrometer. A 5-keV electron beam with a beam current of from 0.3 to 1 μA was used as the excitation source. Si samples were mounted by attaching the Cu wire lead to the sample holder, and Pt samples were clipped down to ensure electrical grounding. The pressure was maintained at $<10^{-8}$ Torr during analysis. A 3-keV electron beam was used in a few samples where charging was a problem.

Depth profiling using an Auger spectrometer has been previously described.[14] A Physical Electronics Model 04-303 differential ion gun was used to produce a 2-keV Ar^+ ion beam for sputtering. The pressure was maintained at $\sim 3 \times 10^{-7}$ Torr in the main vacuum chamber and 1.5×10^{-4} Torr of Ar in the ionization chamber. Generally, signals for C, N, O, Si, the counterion of $(PQ^{2+})_n$, and the substrate (Si or Pt) were analyzed as a function of sputtering time.[15] The energy window used was typically 10-50 eV around the energy characteristic of the element being analyzed. The Auger signals (and their energies) monitored during depth profiles are as follows: C (273 eV), N (379 eV), O (503 eV), Cl (181 eV), S (152 eV), Si (1619 eV), Br (1396 eV), I (511 and 520 eV), and Pt (1967 eV).

Results and Discussion

a. Correlation of Auger Spectroscopic and Electrochemical Analysis of Electrostatically Bound Anions: Binding of $IrCl_6^{2-}$.

Pt electrodes bearing $\sim 10^{-8}$ mol/cm^2 of $(PQ^{2+}\cdot 2Br^-)$ exhibit essentially reversible reduction of the $(PQ^{2+})_n$ at -0.5 V vs. SCE in 0.1 M K_2SO_4 solution. If K_2IrCl_6 is introduced into the solution, an additional redox system is detectable by cyclic voltammetry at ~+0.6 V vs. SCE that is attributable to the $IrCl_6^{2-/3-}$ redox couple. At concentrations of $IrCl_6^{2-}$ where no $IrCl_6^{2-/3-}$ cyclic voltammetry wave is detectable for a naked electrode (1-50 μM) we observe a wave for electrodes bearing $\sim 10^{-8}$ mol/cm^2 of PQ^{2+}. We thus conclude, as was concluded previously for polyvinylpyridinium,[1-3] that the $(PQ^{2+})_n$ can electrostatically bind $IrCl_6^{2-}$ resulting in an electrochemical response that would otherwise be

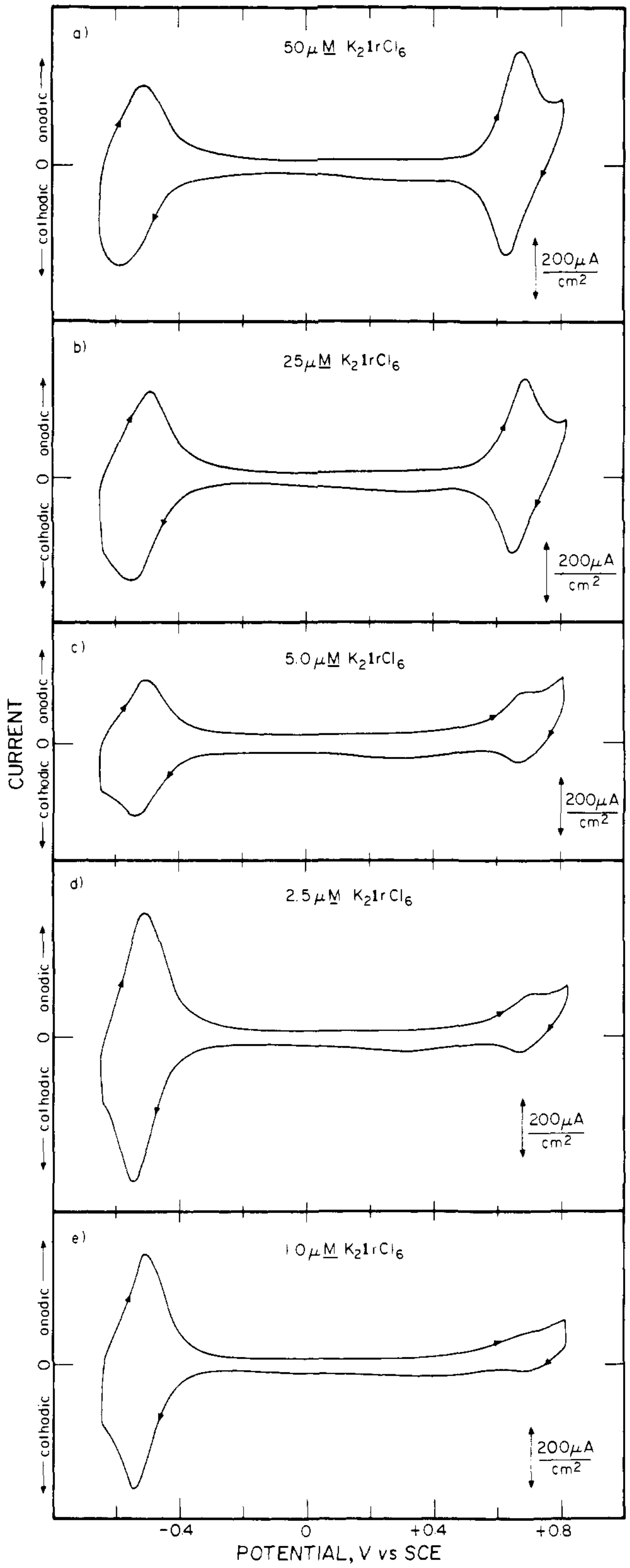

Figure 1. Cyclic voltammograms (100 mV/s) of a Pt/$(PQ^{2+})_n$ electrode in solutions containing 0.1 M K_2SO_4 and (a) 50 μM K_2IrCl_6, (b) 25 μM K_2IrCl_6, (c) 5.0 μM K_2IrCl_6, (d) 2.5 μM K_2IrCl_6, and (e) 1.0 μM K_2IrCl_6. The coverage of electroactive $(PQ^{2+/+\cdot})_n$ is 7.6×10^{-9} mol/cm^2 for (a) and (b), 5.0×10^{-9} mol/cm^2 for (c), and 7.3×10^{-9} mol for (d) and (e). cf. also Table I.

---

(13) Lenhard, J. R.; Murray, R. W. *J. Electroanal. Chem.* **1977**, *78*, 195.

(14) (a) Palmberg, P. W. *J. Vac. Sci. Technol.* **1972**, *9*, 160. (b) Holloway, D. M. *Ibid.* **1975**, *12*, 392. (c) Davis, R. E.; Faulkner, L. R. *J. Electrochem. Soc.* **1981**, *128*, 1349.

(15) Davis, L. E.; MacDonald, N. C.; Palmberg, P. W.; Riach, G. E.; Weber, R. G. "Handbook of Auger Electron Spectroscopy", 2nd ed.; Physical Electronics Division, Perkin-Elmer Corp.: Eden Prairie, MN, 1976.

Table I. Concentration Dependence of Electrostatic Binding of $IrCl_6^{3-}$ to $Pt/(PQ^{2+}\cdot{}^2/_3xIrCl_6^{3-} + (1-x)SO_4^{2-})_n$

		$(PQ^{2+})_n \rightleftarrows (PQ^{+\cdot})_n$		$IrCl_6^{2-} \rightleftarrows IrCl_6^{3-}$		
electrode[a]	$[K_2IrCl_6]$,[b] μM	$E°'$, V vs. SCE[c]	coverage, mol/cm^2 [d]	$E°'$, V vs. SCE[c]	coverage, mol/cm^2 [d]	x
a	50	−0.54	7.3×10^{-9}	+0.66	5.1×10^{-9}	1.0
	0	−0.51	7.3×10^{-9}			0.0
b	25	−0.53	7.3×10^{-9}	+0.66	3.9×10^{-9}	0.8
	0	−0.51	7.3×10^{-9}			0.0
c	5.0	−0.53	5.0×10^{-9}	+0.68	1.8×10^{-9}	0.5
	0	−0.51	5.0×10^{-9}			0.0
d	2.5	−0.53	7.6×10^{-9}	+0.69	1.1×10^{-9}	0.2
	0	−0.51	7.6×10^{-9}			0.0
e	1.0	−0.53	7.6×10^{-9}	+0.68	0.5×10^{-9}	0.1
	0	−0.51	7.6×10^{-9}			0.0

[a] Electrodes a–e are those characterized by the cyclic voltammetry scans in Figure 1, a–e, respectively. Each electrode is thus an independent experiment. [b] Bulk solution (~25 mL) concentration. [c] Average position of the oxidation and reduction current peak for the surface confined species. [d] Coverage of electrochemically active material from integration of cyclic voltammetry wave divided by electrode area. Note that the $IrCl_6^{2-/3-}$ is actually bound as $IrCl_6^{3-}$ since the electrode is held between $E°'(PQ^{2+/+\cdot})_n$ and $E°'(IrCl_6^{2-/3-})$; cf. text. Coverages are ±10%; error is due to inability to accurately subtract background currents.

undetectable. Figure 1 shows cyclic voltammograms for five different electrodes bearing about the same amount of $(PQ^{2+})_n$ in 0.1 M K_2SO_4 solution but with a different concentration of $IrCl_6^{2-}$ in solution in each case. The signal for $IrCl_6^{2-} \rightleftarrows IrCl_6^{3-}$ grows from zero to the value shown in 10–15 min. The data in Figure 1 are representative for this system and are believed to reflect the equilibrium amount of $IrCl_6^{3-}$ electrostatically bound in $(PQ^{2+})_n$. While $IrCl_6^{2-}$ is present in the bulk, the species actually bound is $IrCl_6^{3-}$ because the electrodes were held at a potential sufficiently negative to reduce the $IrCl_6^{2-}$. Thus, eq 4 represents

$$\text{surface-}(PQ^{2+}\cdot SO_4^{2-})_n + {}^2/_3xnIrCl_6^{3-} \rightleftarrows \text{surface-}(PQ^{2+}\cdot{}^2/_3xIrCl_6^{3-} + (1-x)SO_4^{2-})_n + xnSO_4^{2-} \quad (4)$$

the ion-exchange reaction. By integrating the cyclic voltammetry waves, the value of x is determined to vary from ~0.1 up to ~1.0 (Table I), depending on the bulk concentration of $IrCl_6^{2-}$. At very low concentrations of $IrCl_6^{2-}$ there might be some concern as to whether there is significant depletion of the bulk $IrCl_6^{2-}$. For ~25 mL solutions of the 1 μM $IrCl_6^{2-}$ there is a total reservoir of ~25 nmol of $IrCl_6^{2-}$; for $x = 1.0$ this would represent a diminution in the reservoir of $IrCl_6^{2-}$ by less than 25%, since the electrode bears only 7.6 nmol of PQ^{2+}. That the amount of $IrCl_6^{3-}$ in the electrode is the equilibrium amount is established by showing that an electrode where $x = 1.0$ initially changes in time to a value consistent with the bulk $IrCl_6^{2-}$ concentration associated with the solution contacting the electrode. Thus, the same eventual amount of $IrCl_6^{3-}$ is attained at given bulk concentration of $IrCl_6^{2-}$, independent of the initial value of x, for a fixed K_2SO_4 concentration. The time scale of the equilibrium, however, can be quite long, requiring >15 min in some cases.

Two, more subtle, observations tend to confirm the conclusion that $SO_4^{2-}/IrCl_6^{2-/3-}$ equilibration does occur. First, note that $IrCl_6^{2-}$ can be introduced as the 2− species by not potentiostatting the electrode. In the 50 μM $IrCl_6^{2-}$ solution we find that the area under the wave for $IrCl_6^{2-} \rightleftarrows IrCl_6^{3-}$ is initially very close to that under the wave for $(PQ^{2+})_n \rightleftarrows (PQ^{+\cdot})_n$, when the nonpotentiostatted electrode is equilibrated with the solution. However, holding the electrode between $E°'(PQ^{2+/+\cdot})_n$ and $E°'(IrCl_6^{2-/3-})$ for a few minutes and then scanning to determine the amount of surface-confined $IrCl_6^{2-} \rightleftarrows IrCl_6^{3-}$ reveals a diminution in the area under the wave for $IrCl_6^{2-} \rightleftarrows IrCl_6^{3-}$ to a value consistent with the binding of $IrCl_6^{3-}$ to an extent that the positive charge of the $(PQ^{2+})_n$ is fully compensated. It is reasonable that if $IrCl_6^{2-}$ is bound to the fullest extent at 50 μM, then $IrCl_6^{3-}$ would be bound just as well, if not better, since it bears a higher negative charge. The second observation concerns the effect from putting a $Pt/(PQ^{2+}\cdot{}^2/_3IrCl_6^{3-})_n$ electrode at a potential of ~−0.65 V vs. SCE, where the surface-$(PQ^{2+})_n$ is put in the reduced state $(PQ^{+\cdot})_n$, in a solution containing 50 μM $IrCl_6^{2-}$. The first several scans to determine surface $IrCl_6^{3-}$ show the approximately 50% diminution of the signal for $IrCl_6^{2-} \rightleftarrows IrCl_6^{3-}$ expected from the reduction in positive charge of the polymer. These two experiments show that $IrCl_6^{2-/3-}$ can move in and out of the $(PQ^{2+})_n$ layer with sufficient facility that equilibrium with the solution ions can be established.

Two additional points should be made here. First, the cyclic voltammetry is not useful in establishing whether there is additional electrolyte in the surface layer beyond that associated with charge compensation of the $(PQ^{2+})_n$. For example, there may be K_2SO_4 present in the polymer layer. Since reasonable electrochemical responses are observed for the $(PQ^{2+/+\cdot})_n$ and for surface-confined $IrCl_6^{2-/3-}$, the presence of H_2O in the polymer layer is certain. But whether K_2SO_4 is present in the layer is unclear. It is unlikely that excess electrolyte can be excluded, and indeed it may be that K^+ and SO_4^{2-} are the most mobile ions when there is as much $IrCl_6^{2-/3-}$ as PQ^{2+} in the polymer layer. In any event, the local concentration of ions in the polymer layer far exceeds the bulk concentration even when the bulk concentration of electrolyte is 0.1 M. In the absence of a firmly bound anion such as $IrCl_6^{3-}$, the supporting electrolyte charge compensates the polymer, thereby enhancing the electrolyte concentration near the electrode. When a firmly bound anion is present the concentration of supporting electrolyte may, in fact, be smaller than in solution, but the total ion concentration in the region near the electrode is always higher when the polymer is present. The second point of importance is that the extent to which $IrCl_6^{2-/3-}$ will be preent in the surface polymer depends on the other ions present in the solution. This will be elaborated more fully below, but it should be noted here that there are more and less competitive anions than SO_4^{2-}.

The electrodes characterized by the data in Figure 1 and Table I were studied further by Auger spectroscopy, to establish a quantitative correlation between the electrochemically detected $IrCl_6^{2-/3-}$ and Auger signals characteristic of the $IrCl_6^{2-/3-}$. Electrodes were removed from the solutions containing the various $IrCl_6^{2-}$ concentrations and washed with distilled, deionized H_2O. The five electrodes having variable $IrCl_6^{3-}$ content presumably have the surface $(PQ^{2+}\cdot{}^2/_3xIrCl_6^{3-}\cdot(1-x)SO_4^{2-})$ composition present in the electrolyte solution from which each was withdrawn, except for the complication of the unknown K_2SO_4 content. The Auger spectra of the electrodes show signals for C, N, Si, and O that are expected for $(PQ^{2+})_n$ (Figure 2), and additional signals are present in the spectrum that are attributable to the elements S (from SO_4^{2-}) and Ir and Cl (from $IrCl_6^{3-}$) depending on the solution from which the surface is withdrawn. No additional signals are observed, and, in particular, we find little or no detectable signal for K (252 eV) (from K^+). Any K_2SO_4 in the polymer is likely washed away during rinsing with H_2O following removal from the K_2IrCl_6/K_2SO_4 solution. For each electrode the ratio of the N signal to the C signal is the same, ±20%, but the Cl to C ratio varies in a smooth fashion depending on the concentration of $IrCl_6^{2-}$ in the solution from which the electrode was withdrawn (Figure 3). The correlation in Figure 3 is also with the data in Figure 1 that gives the ratio of electroactive, surface-confined $PQ^{2+/+\cdot}$ and $IrCl_6^{2-/3-}$. As shown in Figure 3

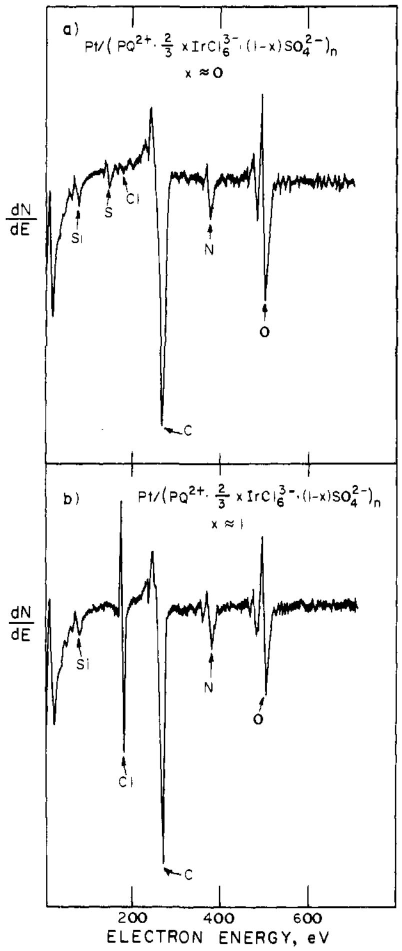

Figure 2. Auger spectra for Pt/$(PQ^{2+}\cdot{}^2/_3xIrCl_6^{3-} + (1 - x)SO_4^{2-})_n$ electrodes. In (a) the electrode was withdrawn from a solution containing 0.1 M K_2SO_4 and 1 μM K_2IrCl_6 and is the electrode characterized by cyclic voltammetry in Figure 1e. In (b) the electrode was withdrawn from a solution containing 0.1 M K_2SO_4 and 50 μM K_2IrCl_6 and is the electrode characterized by cyclic voltammetry in Figure 1a. Each electrode was washed with H_2O prior to the Auger determination and the surfaces were not sputtered. Note that the $IrCl_6^{3-}$, not $IrCl_6^{2-}$, is surface-confined, since the electrode was removed after electrochemical equilibration at a potential between $E°'(PQ^{2+/+\cdot})_n$ and $E°'(IrCl_6^{2-/3-})$.

there is excellent internal consistency between the in situ electrochemical determination of $IrCl_6^{2-/3-}$ and the Auger determination of a washed and dried surface taken from the electrolyte solution. Thus, we can associate particular Cl/C ratios from auger spectroscopy with a particular fractional incorporation of electroactive $IrCl_6^{3-/2-}$.

In our earlier work[11] we showed by Auger spectroscopy that the replacement of Br^- by Cl^- according to eq 5 occurs to an extent

$$(PQ^{2+}\cdot 2Br^-)_n \xrightarrow[\text{aq KCl}]{} (PQ^{2+}\cdot 2Cl^-)_n + 2nKBr \tag{5}$$

that no Br^- is detectable by Auger spectroscopy. For such a surface, the Cl/C ratio is less than for $(PQ^{2+}\cdot PtCl_6^{2-})_n$ by an amount that about reflects the factor of 3 lower Cl content. The Cl/C ratio for an electrode prepared according to eq 6 likewise

$$(PQ^{2+}\cdot 2Br^-)_n \xrightarrow[\text{5 mM } K_2IrCl_6]{} (PQ^{2+}\cdot IrCl_6^{2-})_n + 2nKBr \tag{6}$$

is about a factor of 3 greater than for surface-$(PQ^{2+}\cdot 2Cl^-)_n$. The difference with the $IrCl_6^{2-}$ is that we can know the amount of electroactive $IrCl_6^{2-/3-}$ that is present, in contrast to $PtCl_6^{2-}$ which does not exhibit reversible electrochemistry. Since the $IrCl_6^{2-}$ is very similar to $PtCl_6^{2-}$ in size and charge, the behavior of $IrCl_6^{2-}$ is expected to be close to that for $PtCl_6^{2-}$ in terms of incorporation into $(PQ^{2+})_n$ when competing against other anions.

Auger spectroscopic analysis of electrode surfaces bearing $(PQ^{2+})_n$ and the charge compensating anions reveal the surfaces to be reasonably free of detectable contaminants. At least we do not observe signals for extraneous elements and the elements that are expected to be present are detectable. One additional check of internal consistency comes from monitoring the Auger signal intensity for the various detectable elements while sputtering away the exposed surface with a beam of reactive Ar ions. This so-called depth profile analysis gives information concerning the elemental composition of the electrode/polymer interface as a function of depth in the polymer. A typical set of depth profile analyses is given in Figure 4. Note that substrate Pt signals overlap those for N; Si and N are low-sensitivity elements. These facts account for the nearly independent signal intensity for N and Si as a

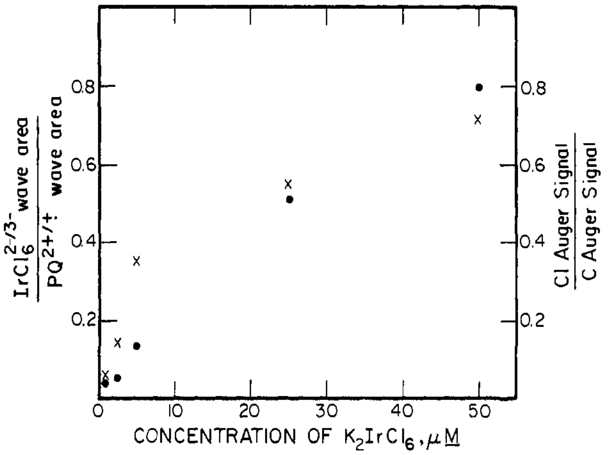

Figure 3. A graph comparing electrochemical and auger data for Pt/$(PQ^{2+}\cdot{}^2/_3xIrCl_6^{3-} + (1 - x)SO_4^{2-})_n$ electrodes. The cyclic voltammetry of these electrodes is shown in Figure 1. The scale on the left-hand side refers to the ratio of the integrated areas of the $IrCl_6^{2-/3-}$ and $(PQ^{2+/+\cdot})_n$ waves, in solutions containing the appropriate concentrations of K_2IrCl_6 (X). The scale on the right-hand side refers to the ratio of Auger signals obtained for C and Cl on these same electrodes (●) without sputtering. Auger spectra for $[IrCl_6^{2-}]$ = 1 and 50 μM are shown in Figure 2. Auger signal intensities have not been corrected for element sensitivity.

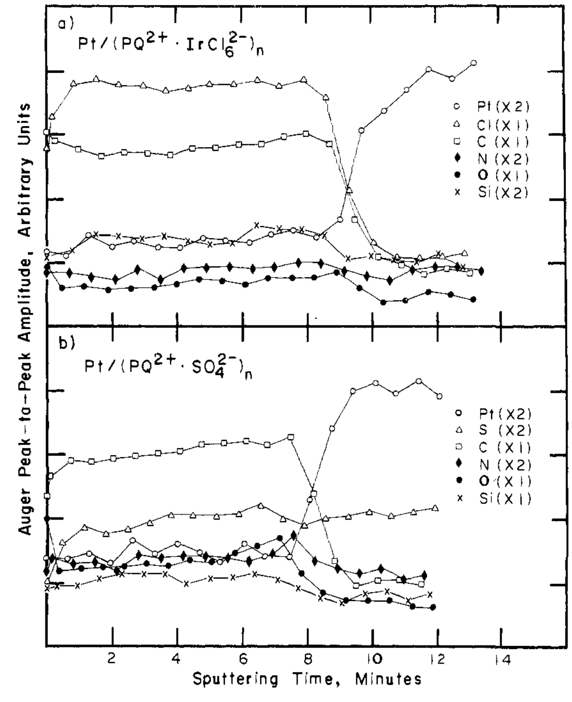

Figure 4. Auger/depth profile analysis of Pt/$(PQ^{2+}\cdot xIrCl_6^{2-} + (1 - x)SO_4^{2-})_n$ electrodes. The electrode characterized in (a) was withdrawn from a solution of 5 mM K_2IrCl_6 and that in (b) was withdrawn from a solution of 0.1 M K_2SO_4. In (a) $x \approx 1$ and in (b) $x \approx 0$. Electrodes were washed with H_2O prior to Auger analysis. Note that low-energy Pt signals interfere with the low-energy signals characteristic of other elements, especially S.

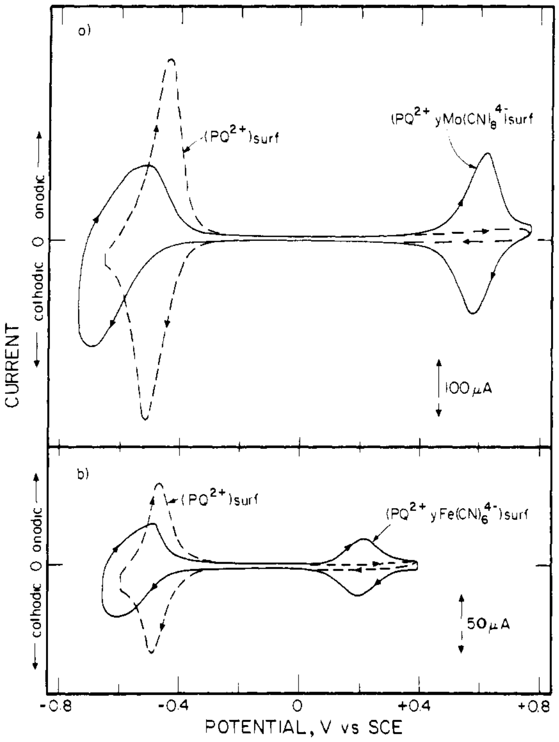

Figure 5. Cyclic voltammograms (100 mV/s) in 0.1 M KCl of (a) a $Pt/(PQ^{2+}\cdot{}^1/_2Mo(CN)_8{}^{4-})_n$ electrode prepared by immersing a $Pt/(PQ^{2+})_n$ electrode into ~5 mM $K_4Mo(CN)_8/H_2O$, and then rinsing, and (b) a $Pt/(PQ^{2+}\cdot{}^1/_2Fe(CN)_6{}^{4-})_n$ electrode prepared as in (a) except using $K_4Fe(CN)_6$. The coverage of electroactive $(PQ^{2+/+\cdot})_n$ is 1.3×10^{-8} mol/cm^2 for (a) and 3.7×10^{-9} mol/cm^2 for (b).

function of sputtering time. Generally, there is some variation in element ratios near the surface, as detected by the changing Auger signal intensity as the sputtering time increases. But within a short time, it would appear that the polymer layer, bearing different anions, does have constant composition. The Auger signal intensities without sputtering may thus be suspect, since these may not always accurately reflect the composition of the bulk of the polymer. On the other hand, the sputtering technique itself is a destructive one and can lead to selective removal of various substances as the surface suffers damage from both the Auger exciting beam and the Ar ion sputtering beam.[16] We generally find good qualitative agreement for Auger analyses with and without sputtering in the sense that selective anion binding can be determined to occur (Figures 2 and 4). However, as is well appreciated by other workers using Auger spectroscopy, the quantitative determination of element ratios by Auger spectroscopy will not be as good as an elemental analysis from combustion analyses. We find very reasonable reproducibility and would estimate an error of less than ±30% in determining the ratio of compensating anions in $(PQ^{2+})_n$ when taking ratios from depth profile analyses.

b. Electrostatic Binding of Electroactive Transition Metal Cyanide Complexes. The incorporation of the electroactive $IrCl_6{}^{2-/3-}$ system into $(PQ^{2+})_n$ prompted us to examine the electrostatic binding of other negatively charged metal complexes. One large class of such complexes are the transition metal cyanides, a number of which can, in fact, be isolated in at least two oxidation states. We have thus examined the behavior of $Co(CN)_6{}^{3-}$, $Fe(CN)_6{}^{3-}$, $Fe(CN)_6{}^{4-}$, $Ru(CN)_6{}^{4-}$, and $Mo(CN)_8{}^{4-}$ as represenatative of this class. Of these, only $Co(CN)_6{}^{3-}$ does not exhibit reversible electrochemical behavior.

The metal cyanide complexes bind strongly to the $(PQ^{2+})_n$. Figure 5 shows typical electrochemical behavior of Pt electrodes derivatized with I before and after incorporation of $Fe(CN)_6{}^{4-}$ or $Mo(CN)_8{}^{4-}$. Incorporation of the metal complex was brought about by dipping the unpotentiostated $(PQ^{2+}\cdot 2Br^-)_n$ coated electrodes into an aqueous ~5 mM solution of the appropriate complex as the K^+ salt for ~5 min. The electrode was then removed, washed, and reexamined by cyclic voltammetry in 0.1 M KCl to determine whether any electroactive complex was retained. As shown in Figure 4 cyclic voltammetry waves having an area of ca. one-half of that for the $(PQ^{2+})_n \rightleftarrows (PQ^{+}\cdot)_n$ are initially observed after replacment of Cl^- by $Mo(CN)_8{}^{4-}$ or $Fe(CN)_6{}^{4-}$. This ~1:2 ratio is that expected for complete compensation of charge by the complexes. The waves for the electrostatically bound anions do diminish with time in 0.1 M KCl, but even after 4 h detectable waves still obtain. For finite volumes of electrolyte solution it is apparent that there can be measurable amounts of the complex anions that persist in the polymer at equilibrium.

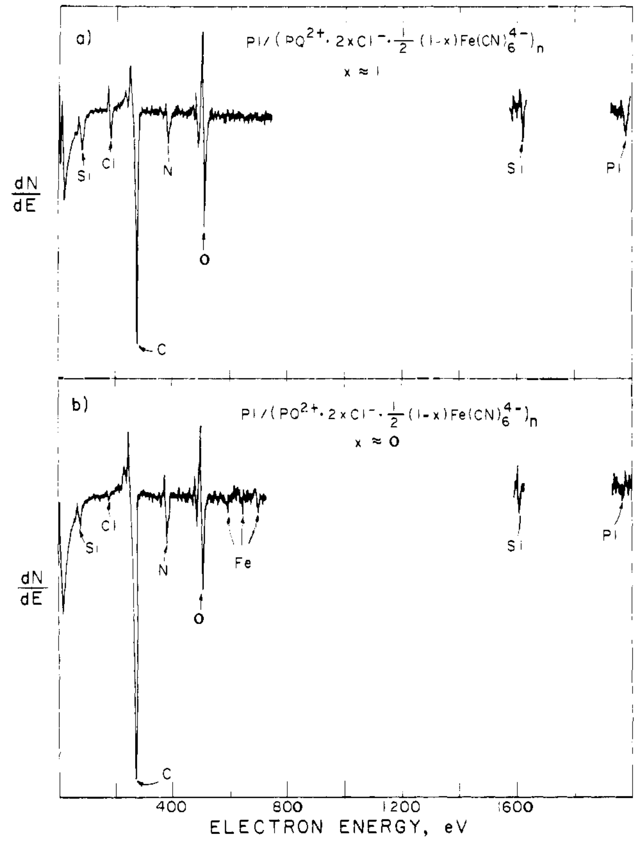

Figure 6. Auger spectral analysis of $Pt/(PQ^{2+}\cdot 2xCl^-\cdot{}^1/_2(1-x)Fe(CN)_6{}^{4-})_n$. In (a) the electrode was withdrawn from 0.1 M KCl, 1 μM $K_4Fe(CN)_6$, $x \approx 1$; and in (b) the electrode was withdrawn from 0.1 M KCl, 100 μM $K_4Fe(CN)_6$, $x \approx 0$. Electrodes were washed prior to auger analysis but were not sputtered.

As for electrodes bearing $(PQ^{2+})_n$ into which $IrCl_6{}^{2-}$ is incorporated (Figure 4), we have recorded Auger spectra for unpotentiostated Pt electrodes bearing $(PQ^{2+})_n$ that have been withdrawn, and subsequently washed, from solutions containing variable amounts of $K_4Fe(CN)_6$ and a fixed concentration of KCl. Auger spectra for a pair of electrodes are given in Figure 6. As expected, the Cl signal associated with the $(PQ^{2+}\cdot 2Cl^-)_n$ is attenuated for the electrode withdrawn from the solution containing the higher $Fe(CN)_6{}^{4-}$ concentration. When incorporated (Figure 6b), $Fe(CN)_6{}^{4-}$ bound to the $(PQ^{2+})_n$ exhibits a signal characteristic of Fe. Moreover, there is a definite change in the C/N ratio in accord with a high relative N concentration in $(PQ^{2+}\cdot{}^1/_2Fe(CN)_6{}^{4-})_n$ compared to $(PQ^{2+}\cdot 2Cl^-)_n$. The data in Figure 6 provide further substantiation of the Auger spectroscopic technique as a method to determine the relative binding of one anion compared with another. For all of the transition metal complexes that we have investigated, $MCl_6{}^{2-}$ (M = Pt, Ir); $M(CN)_x{}^{n-}$ (M = Co, Fe, Ru, Mo), we find that only small con-

---

[16] (a) Chang, C. C. *Surf. Sci.* **1971**, *25*, 53. (b) Van Oostrom, A. *J. Vac. Sci. Technol.* **1976**, *13*, 224.

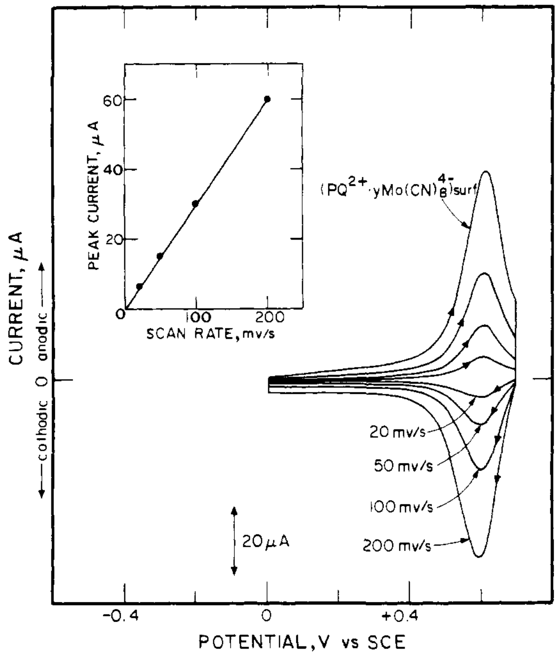

Figure 7. Cyclic voltammograms for a Pt/$(PQ^{2+}\cdot{}^1/_2Mo(CN)_8{}^{4-})_n$ electrode in 0.1 M KCl/H_2O at different scan rates. The inset shows that the peak current for the $Mo(CN)_8{}^{4-/3-}$ wave varies linearly with the scan rate, as expecte for a reversible, surface-attached species. The coverage of electroactive $(PQ^{2+})_n$ is 1×10^{-9} mol/cm^2.

centrations are required to completely displace the small inorganic anions such as X^- (X = Cl, Br, I, NCS, ClO_4) or $SO_4{}^{2-}$ from the $(PQ^{2+})_n$ on the surface, even when the small anions are present at significant (~0.1 M) bulk concentration. Auger and electrochemical measurements have been employed to draw this conclusion. In sections c and d below, we detail the procedures for ordering the binding of the anions.

The metal cyanides studied are not substitution labile and likely remain intact upon binding to the $(PQ^{2+})_n$. We find that in aqueous 0.1 M KCl the positions of the cyclic voltammetry waves are close to those found when the complexes are examined at the naked electrode surfaces (Table II). Thus, like the $IrCl_6{}^{2-/3-}$ system, the metal cyanides can be incorporated into the polymer with relatively little perturbation of the electrochemistry. The kinetics for the surface-confined species have not been studied in detail, but Figure 7 shows the variation of the cyclic voltammograms for electrostatically bound $Mo(CN)_8{}^{4-}$, illustrating that the $Mo(CN)_8{}^{3-} \rightleftarrows Mo(CN)_8{}^{4-}$ process is sufficiently fast to give the expected linear response of peak current with scan rate up to 200 mV/s. Data represented by Figure 7 for $Mo(CN)_8{}^{3-/4-}$ are representative of that for other electrostatically bound anions that are electroactive.

The effect of the anion on the electrochemical response of the $(PQ^{2+})_n \rightleftarrows (PQ^{+\cdot})_n$ system is quite noticeable (Figure 5). The tightly bound anions ($Co(CN)_6{}^{3-}$, $Fe(CN)_6{}^{3-/4-}$, $Ru(CN)_6{}^{3-/4-}$, $Mo(CN)_8{}^{3-/4-}$, and $IrCl_6{}^{2-/3-}$) tend to broaden the wave and shift the average position of the oxidation and reduction current peaks to somewhat more negative potentials. The kinetics for the $(PQ^{2+})_n \rightleftarrows (PQ^{+\cdot})_n$ are also worsened by the incorporation of the tightly bound anions as reflected in the appearance of the cyclic voltammograms at scan rates exceeding 100 mV/s; the peak-to-peak separation increases and the waves appear broader. It is interesting that the electrochemical response to the metal complex is as good as it is, while the kinetics of the $(PQ^{2+})_n$ system suffer upon incorporation of the anion.

The electrochemical behavior of Pt electrodes bearing species such as $(PQ^{2+}\cdot{}^1/_2Fe(CN)_6{}^{4-})_n$ is not unexpectedly, dependent on the solvent. Since $E°'(Fe(CN)_6{}^{3-/4-})$ is dependent on solvent,[17] we felt that this sensitivity to solvent could be exploited to reveal the solvent composition inside the polymer layer compared to the bulk. Changing the solvent from H_2O to CH_3CN does have a profound effect on *both* the behavior of the $(PQ^{2+})_n \rightleftarrows (PQ^{+\cdot})_n$ and $Fe(CN)_6{}^{3-} \rightleftarrows Fe(CN)_6{}^{4-}$ systems. The $Fe(CN)_6{}^{3-/4-}$ wave is shifted more negative, broadened, and like the $(PQ^{2+/+\cdot})_n$ wave appears to be reduced in total area. Similar effects are found for the $(PQ^{2+}\cdot{}^1/_2Mo(CN)_8{}^{4-})_n$. The poor electrochemical response in CH_3CN is found with 0.1 M $[n\text{-}Bu_4N]ClO_4$, $LiClO_4$, or $[Et_4N]Cl$ as supporting electrolyte. In all cases it would appear that the solvation by CH_3CN is so poor that the electrochemical behavior of the surface groups is drastically worse. Changing from H_2O to CH_3CN solvent for a system such as $(PQ^{2+}\cdot 2Cl^-)_n$ on Pt only modestly affects the electrochemical response of the $(PQ^{2+/+\cdot})_n$ at cyclic voltammetry scan rates of ~100 mV/s. It would thus appear that the deleterious effects from CH_3CN as solvent can be attributed to the tight ion pairing of $(PQ^{2+})_n$ with the large anionic complexes. Interestingly, it would appear that only small amounts of H_2O added to CH_3CN (<5% by volume) are required to essentially regenerate the electrochemical properties found in pure H_2O solvent. The $(PQ^{2+}\cdot\text{complex anion})_n$ may concentrate the H_2O beyond the bulk concentration, since H_2O may solvate the ion pairs much more strongly.

Since the complex anions are persistently electrostatically bound to $(PQ^{2+})_n$ in solutions of 0.1 M KCl that contain no added complex anion, it is logical to conclude that the rate of loss of the complex is slow and that there is only slow movement of the complex anions in and out of the $(PQ^{2+})_n$ as the electrode is cycled between $(PQ^{2+})_n$ and $(PQ^{+\cdot})_n$. In these situations the essential charge neutrality of the polymer layer must be brought about by the movement of the cations, say K^+, in and out of the layer. Thus, relatively fast $(PQ^{2+})_n \rightleftarrows (PQ^{+\cdot})_n$ interconversion or redox cycling of the complex anion may depend on the cation mobility when there are complex anions tightly bound to the $(PQ^{2+/+\cdot})_n$ layer. As for $IrCl_6{}^{2-/3-}$, though, holding the polymer layer in the reduced state, $(PQ^{+\cdot})_n$, will result in the eventual extrusion of the proper fraction of complex anion. A saturated solution of KCl will more rapidly lead to the diminution of the electrochemical response to the electrostatically bound anion.

c. Ordering the Binding of Complex Anions. As indicated above, the transition metal complex anions are much more firmly bound than the simple inorganic anions. In this section we describe results establishing the relative ordering of complex anion binding to $(PQ^{2+})_n$. To illustrate the issue we can ask whether $IrCl_6{}^{2-}$ or $Fe(CN)_6{}^{4-}$ will be the charge compensating ion for $(PQ^{2+})_n$ when the solution contains both $IrCl_6{}^{2-}$ and $Fe(CN)_6{}^{4-}$. To answer such a question we exploit the fact that both ions are reversibly electroactive and examine the electrochemical response of a $(PQ^{2+})_n$-coated Pt electrode in a solution containing 0.1 M KCl, 50 μM K_2IrCl_6, and 50 μM $K_4Fe(CN)_6$. The potential range scanned is such that $(PQ^{2+})_n$ remains in the oxidized (2+) state. Initially, cyclic voltammetry waves are observed for the $Fe(CN)_6{}^{3-} \rightleftarrows Fe(CN)_6{}^{4-}$ and for the $IrCl_6{}^{2-} \rightleftarrows IrCl_6{}^{3-}$ systems. However, eventually the signal for the Ir system vanishes while the signal for the Fe system increases until the cyclic voltammetry shows that the charge associated with $(PQ^{2+})_n$ is completely neutralized by the electroactive $Fe(CN)_6{}^{4-}$. Thus, we conclude that both $IrCl_6{}^{2-}$ and $Fe(CN)_6{}^{4-}$ can quickly go into the polymer, but the thermodynamics are such that $Fe(CN)_6{}^{4-}$ is significantly more firmly bound. Likewise, examining the electrochemical response of a $(PQ^{2+})_n$-coated electrode after ~15 min equilibrium (nonpotentiostatted) in 0.1 M KCl, 50 μM K_2IrCl_6, and 50 μM $K_4Fe(CN)_6$ shows waves for only the $Fe(CN)_6{}^{3-/4-}$ couple.

Examination of the electrochemical response of a $(PQ^{2+})_n$-coated Pt electrode in 0.1 M KCl, 50 μM $K_4Fe(CN)_6$, and 50 μM $K_4Mo(CN)_8$ initially reveals cyclic voltammetry signals for both the Fe and Mo systems. During the first few cyclic voltammetry scans the signal for the Fe and the Mo systems both grow, but the signal for Fe grows faster. This suggests that the $Fe(CN)_6{}^{4-}$ is more mobile that $Mo(CN)_8{}^{4-}$. Eventually, the signal for the Fe system declines while the Mo signal slowly grows to reflect a very high $Mo(CN)_8{}^{4-}/Fe(CN)_6{}^{4-}$ ratio bound to $(PQ^{2+})_n$.

---

(17) Noufi, R.; Tench, D.; Warren, L. F. *J. Electrochem. Soc.* **1980**, *127*, 2709.

Table II. Electrochemical Potential of Aqueous and Electrostatically Bound Complex Anions

complex	$E°'$, V vs. SCE[a] solution	$E°'$, V vs. SCE[a] bound to $(PQ^{2+})_n$
$Fe(CN)_6^{3-/4-}$	+0.19 ± 0.02	+0.20 ± 0.03
$Ru(CN)_6^{3-/4-}$	+0.70 ± 0.02	+0.68 ± 0.03
$Mo(CN)_8^{3-/4-}$	+0.57 ± 0.02	+0.60 ± 0.03
$IrCl_6^{2-/3-}$	+0.65 ± 0.02	+0.66 ± 0.03

[a] Electrochemical potentials, $E°'$, for the indicated couple dissolved in H_2O at 25 °C or confined to $(PQ^{2+})_n$ measured for Pt electrodes in 0.1 M KCl by cyclic voltammetry. The $E°'$ is taken to be the average of the anodic and cathodic current peaks at a scan rate of 100 mV/s. The coverage of $(PQ^{2+})_n$ is generally in the range $5 \times 10^{-9} - 5 \times 10^{-8}$ mol/cm².

Similar experimentation shows that $Mo(CN)_8^{4-}$ is bound much more firmly than $Ru(CN)_6^{4-}$, while $Ru(CN)_6^{4-}$ is only slightly more firmly bound than $Fe(CN)_6^{4-}$.

The results from cyclic voltammetry of (PQ^{2+})-coated Pt electrodes in the presence of pairs of the electroactive complex anions allows us to establish the ordering of binding:

$$Mo(CN)_8^{4-} > Ru(CN)_6^{4-} \sim Fe(CN)_6^{4-} > IrCl_6^{2-/3-} >> Cl^-$$

$$\xleftarrow[\text{increased binding}]{\hspace{6cm}}$$

Attenuation of the cyclic voltammetry wave for polymer-bound $Fe(CN)_6^{3-} \rightleftarrows Fe(CN)_6^{4-}$ by adding $K_3Co(CN)_6$ to a solution of 0.1 M KCl/50 μM $K_4Fe(CN)_6$ provides evidence for the strong and competitive binding of $Co(CN)_6^{3-}$ even though $Co(CN)_6^{3-}$ is electrochemically silent in the accessible potential range in H_2O. For example, addition of $K_3Co(CN)_6$ to bring its concentration to 25 μM attenuates the signal for the $Fe(CN)_6^{3-/4-}$ couple to ~50% of its initial value; addition of $K_3Co(CN)_6$ to a concentration of 50 μM attenuates the wave for $Fe(CN)_6^{3-/4-}$ even more, to about 30% of its original value. These experiments place $Co(CN)_6^{3-}$ in the vicinity of $Fe(CN)_6^{4-}$ and $Ru(CN)_6^{4-}$. However, $Co(CN)_6^{3-}$ is considerably more weakly bound than $Mo(CN)_8^{4-}$. This conclusion follows from the fact that $Mo(CN)_8^{4-}$ is the dominant polymer-bound electroactive ion when $(PQ^{2+})_n$-coated Pt electrodes are immersed in electrolyte solutions containing equal concentrations of $Fe(CN)_6^{4-}$ and $Mo(CN)_8^{4-}$, whereas $Fe(CN)_6^{4-}$ is still present at significant concentration in the $(PQ^{2+})_n$ when $Fe(CN)_6^{4-}$ and $Co(CN)_6^{3-}$ are in the bulk solution at equal concentration.

The same signal for the $Fe(CN)_6^{3-/4-}$ system is eventually observed if a $(PQ^{2+}\cdot 2Cl^-)_n$-coated electrode is immersed into a 0.1 M KCl solution that contains 50 μM $K_4Fe(CN)_6$ and 50 μM $K_3Co(CN)_6$ as when a $(PQ^{2+}\cdot{}^1/_2Fe(CN)_6^{4-})_n$ electrode is immersed into the same solution. The point is that the same concentration of the surface-bound polymer–anion system, $(PQ^{2+}\cdot xFe(CN)_6^{4-}\cdot yCo(CN)_6^{3-})_n$, is obtained independent of the initial composition of the electrode or the order of addition of reagents. The conclusion is that the $(PQ^{2+})_n$-coated Pt does come into equilibrium with the ions in solution. Similarly, concerning the composition of the bound, electroactive anions $M(CN)_6^{4-}$ (M = Fe, Ru), $Mo(CN)_8^{4-}$, and $IrCl_6^{2-}$, the electrochemical response is eventually independent of the initial distribution of ions in the polymer, and the order of addition of anions to a solution does not alter the distribution of detected anions in the $(PQ^{2+})_n$ layer. Thus, in all cases, our measurements of anion binding are for situations where we are certain that equilibrium has been established; we are not limited by kinetically sluggish ion exchange. Table III summarizes the experimentation discussed so far to establish the ordering of the binding of complex anions, and Figures 8 and 9 illustrate typical cyclic voltammetry data for such experimentation. Comparison of wave shapes in Figures 1, 5, and 7–9 indicate considerable variation. Such variation may be due to the differences in coverage, degree of cross-linking in the

Table III. Electrochemical Experimentation to Establish Ordering of Binding of Complex Anions to $(PQ^{2+})_n$

expt	perturbation	response	conclusion
1	dip $(PQ^{2+}\cdot 2Cl^-)_n$ electrode into 0.1 M KCl/50 μM K_2IrCl_6	$(PQ^{2+/+\cdot})_n$ wave broadens and shifts negative; $IrCl_6^{2-/3-}$ wave grows in until equal in area to $(PQ^{2+/+\cdot})_n$	$IrCl_6^{2-} \gg Cl^-$
2	add $K_4Fe(CN)_6$ to 50 μM in above system	$IrCl_6^{2-/3-}$ wave disappears; $Fe(CN)_6^{3-/4-}$ wave grows to $^1/_2$ of $(PQ^{2+/+\cdot})_n$ wave	$Fe(CN)_6^{4-} > IrCl_6^{2-}$
3	add $K_4Mo(CN)_8$ to 50 μM in above system	$Fe(CN)_6^{3-/4-}$ wave disappears; $Mo(CN)_8^{3-/4-}$ wave appears and grows to $^1/_2$ of $(PQ^{2+/+\cdot})_n$ waves	$Mo(CN)_8^{4-} > Fe(CN)_6^{4-}$
4	add $K_4Ru(CN)_6$ to 50 μM in above system	no change in cyclic voltammograms	$Ru(CN)_6^{4-} < Mo(CN)_8^{4-}$
5	dip electrode from expt 4 into saturated KCl for 5 min and scan in 0.1 M KCl containing no other ions	original response of $(PQ^{2+/+\cdot})_n$ regenerated; no signals detectable for bound complexes	$(PQ^{2+}\cdot 2Cl)_n$ regenerated by ion exchange with excess Cl^-
6	dip $(PQ^{2+}\cdot 2Cl^-)_n$ electrode into 0.1 M KCl/50 μM each of $K_4Fe(CN)_6$, $K_4Ru(CN)_6$, K_2IrCl_6, $K_4Mo(CN)_8$	$(PQ^{2+/+\cdot})_n$ wave broadened and shifted negative; eventual growth of $Mo(CN)_8^{3-/4-}$ to an area of $^1/_2$ of $(PQ^{2+/+\cdot})_n$ wave	binding of $Mo(CN)_8^{4-}$ unaffected by presence of other complexes
7	dip $(PQ^{2+}\cdot 2Cl^-)_n$ electrode into 0.1 M KCl/50 μM K_2IrCl_6/50 μM $K_4Fe(CN)_6$	$(PQ^{2+/+\cdot})_n$ wave broadens and shifts negative; waves for $Fe(CN)_6^{3-/4-}$ and $IrCl_6^{2-/3-}$ initially grow; eventually wave for $IrCl_6^{2-/3-}$ vanishes and $Fe(CN)_6^{3-/4-}$ grows to $^1/_2$ area of $(PQ^{2+/+\cdot})_n$ wave	initial response kinetically controlled; eventual response thermodynamically controlled: $Fe(CN)_6^{4-} > IrCl_6^{2-}$
8	dip $(PQ^{2+}\cdot{}^1/_2Fe(CN)_6^{4-})_n$ electrode into 0.1 M KCl/50 μM $K_4Fe(CN)_6$/50 μM $K_3Co(CN)_6$	wave for $Fe(CN)_6^{3-/4-}$ declines to a value reflecting 70% loss of $Fe(CN)_6^{3-/4-}$	$Co(CN)_6^{3-} > Fe(CN)_6^{4-}$
9	dip $(PQ^{2+}\cdot 2Cl^-)_n$ electrode into 0.1 M KCl/50 μM $K_4Fe(CN)_6$	$Fe(CN)_6^{3-/4-}$ wave grows to an area of $^1/_2$ of that for $(PQ^{2+/+\cdot})_n$ $(PQ^{2+/+\cdot})_n$ wave broadens and shifts more negative	$Fe(CN)_6^{4-} \gg Cl^-$
10	dip $(PQ^{2+}\cdot 2Cl^-)_n$ electrode into 0.1 M KCl/50 μM $K_4Fe(CN)_6$/50 μM $K_3Co(CN)_6$	same cyclic voltammetry as in expt 8	$Co(CN)_6^{3-} > Fe(CN)_6^{4-}$

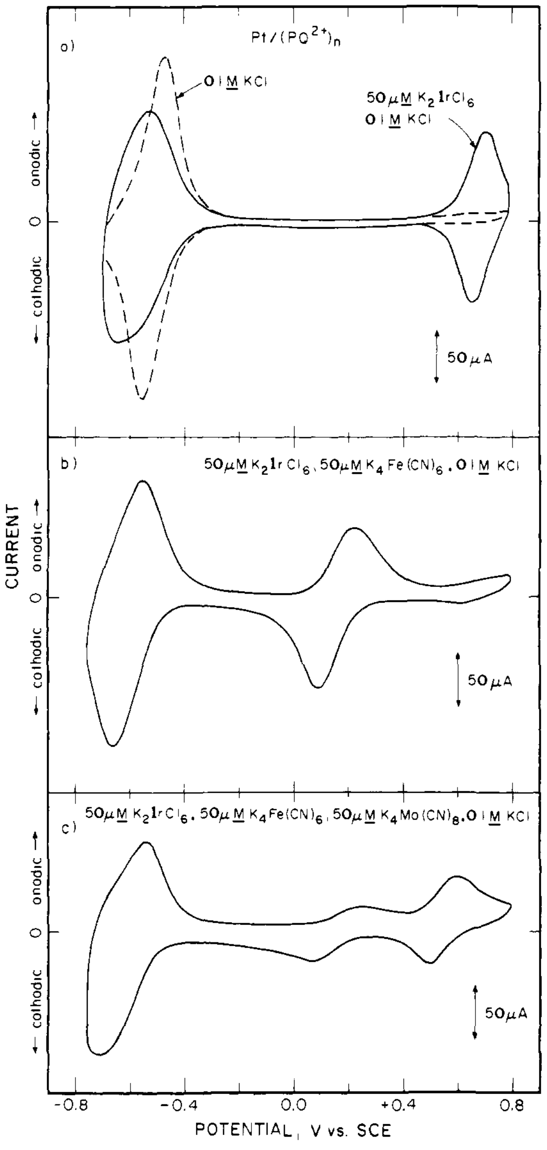

Figure 8. Cyclic voltammograms, 100 mV/s, of a Pt/$(PQ^{2+})_n$ electrode in (a) ---, 0.1 M KCl; —, 0.1 M KCl/50 μM K_2IrCl_6; (b) 0.1 M KCl/50 μM K_2IrCl_6/50 μM $K_4Fe(CN)_6$; (c) 0.1 M KCl/50 μM K_2IrCl_6/50 μM $K_4Fe(CN)_6$/50 μM $K_4Mo(CN)_8$. The coverage of PQ^{2+} is 2.1×10^{-8} mol/cm^2. In each case the unpotentiostatted electrode was equilibrated for ~15 min prior to running the cyclic voltammogram.

polymer, and the nature of the distribution of electroactive complex(es) present in the film.

Auger spectroscopy can also be used to order the binding of the tightly bound transition metal complexes, as illustrated by the spectra given in Figures 2 and 6. Generally, the unique Auger signal for the metal ion of the complex is weak and element ratios are not always easily quantitated. For example, the signal for Fe or Mo when the respective cyanide complexes are bound to $(PQ^{2+})_n$ is very weak relative to the signal for C. Consequently, we have not used Auger spectroscopy to order binding of the tightly bound, electroactive metal complexes.

d. Ordering the Binding of Weakly Bound, Nonelectroactive Anions. Table IV details Auger spectroscopy results that allow us to order the binding of several anions to the $(PQ^{2+})_n$. A typical experiment involves dipping a Pt/$(PQ^{2+}\cdot 2Br^-)_n$ electrode into an aqueous solution containing a one-to-one ratio of two anions. Equilibration at 25 °C for 15 min is generally sufficient to ensure that the anions in the polymer reflect the equilibrium situation. The equilibrated surface is then removed from the solution, washed with distilled H_2O, and then analyzed for the anion by Auger/depth profile analysis.

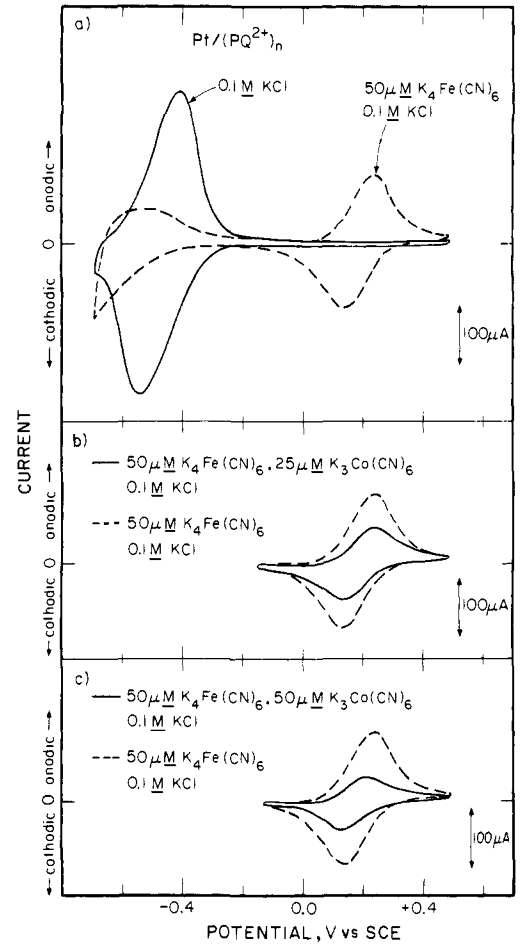

Figure 9. Cyclic voltammograms, 100 mV/s, of a Pt/$(PQ^{2+})_n$ electrode in (a) —, 0.1 M KCl; ---, 0.1 M KCl/50 μM $K_4Fe(CN)_6$; (b) —, 0.1 M KCl/50 μM $K_4Fe(CN)_6$/25 μM $K_3Co(CN)_6$; ---, 0.1 M KCl/50 μM $K_4Fe(CN)_6$; (c) — 0.1 M Kcl/50 μM $K_4Fe(CN)_6$/50 μM $K_3Co(CN)_6$. In (b) and (c) the cyclic voltammograms are the same when starting with either Pt/$(PQ^{2+}\cdot 2Cl^-)_n$ or Pt/$(PQ^{2+}\cdot {}^1/_2Fe(CN)_6{}^{4-})_n$. The coverage of PQ^{2+} is 2.8×10^{-8} mol/cm^2. As for Figure 8, the unpotentiostatted electrode was equilibrated for ~15 min prior to running the cyclic voltammogram.

The series of experiments summarized by the data in Table IV allow the ordering of anions:

$$I^- > SCN^- \sim ClO_4^- \sim SO_4^{2-} > Br^- > Cl^- \sim p\text{-toluenesulfonate}$$

$$\xleftarrow[\text{increasing binding}]{\hspace{8em}}$$

All of the transition metal complex anions are much more firmly bound than these anions. The relative binding spans a range of only about a factor of 10 from I^- to Cl^- in the sense that a solution containing ~10/1 Cl^-/I^- will give a polymer having ~1/1 Cl^-/I^-. In the same sense, $IrCl_6^{2-}$ to SO_4^{2-} spans a range of 10^3–10^4 in that ~20 μM K_2IrCl_6/0.1 M K_2SO_4 yields a polymer having ~1/1 $SO_4^{2-}/IrCl_6^{2-}$.

Given the results of others concerning the electrostatic binding of transition metal complexes to surface-confined polyions, the rather strong binding of the transition metal complexes to $(PQ^{2+})_n$ is not surprising.[1-3] For the weakly bound ions we find that the ions are very labile. Even the strongest of the weakest surface-confined ions, I^-, is labile. Cyclic voltammetry signals apparently associated with $3I^- \rightleftarrows I_3^-$ for Pt/$(PQ^{2+}\cdot 2I^-)_n$ electrodes immersed into 0.1 M KCl last for only a few scans at 100 mV/s, whereas the tightly bound metal complexes give rise to persistent cyclic voltammetry signals. The cyclic voltammetry (100 mV/s) for $(PQ^{2+})_n$ is not significantly dependent on the supporting electrolyte (0.1 M) when a weakly bound anion is used. Thus, a wide range of K^+ or Na^+ salts are useful as the electrolyte for the

Table IV, Auger Signal Intensities for Anions Bound in $(PQ^{2+})_n$[a]

solution[b]	signal intensities, ±30%[c]	conclusion
0.1 M KCl	Cl/C = 0.67	Cl^- bound
0.01 M K_2IrCl_6	Cl/C = 1.4	$IrCl_6^{2-}$ bound
0.1 M KI	I/C ≈ 1.1 (0 signal interferes)[d]	I^- bound
0.10 M K_2SO_4	S/C = 0.32	SO_4^{2-} bound
0.05 M Na(*p*-toluenesulfonate) 0.05 M KCl	S/C = 0.22; Cl/C = 0.20	*p*-toluenesulfonate ≈ Cl^-
0.05 M KCl 0.05 M KBr	Br/C = 0.13; Cl/C = 0.09	$Br^- > Cl^-$
0.05 M KCl 0.05 M KI	I/C ≈ 0.6;[d] Cl/C = 0.02	$I^- > Br^- > Cl^-$
0.09 M KCl 0.01 M KI	I/C ≈ 0.5;[d] Cl/C = 0.28	$I^- > Cl^-$ (factor of ~10)
0.05 M KCl 0.05 M KSCN	S/C = 0.45; Cl/C = 0.02	$SCN^- > Cl^-$
0.05 M KSCN 0.05 M KI	S/C = 0.29; I/C ≈ 0.3[d]	$SCN^- \approx I^-$
0.01 M KSCN 0.01 M $NaClO_4$	S/C = 0.27; Cl/C = 0.59	$ClO_4^- \approx SCN^-$
0.05 M KCl 0.05 M K_2SO_4	S/C = 0.30; Cl/C = 0.04	$SO_4^{2-} > Cl^-$
0.05 M KBr 0.05 M K_2SO_4	S/C = 0.16; Br/C = 0.10	$SO_4^{2-} \approx Br^-$
0.05 M KI 0.05 M K_2SO_4	S/C = 0.05; I/C ≈ 0.6[d]	$I^- > SO_4^{2-}$
0.01 M K_2SO_4 0.01 M $NaClO_4$	S/C = 0.16; Cl/C = 0.16	$SO_4^{2-} \approx ClO_4^-$
1 mM K_2SO_4[e] 1 mM K_2PtCl_6	S/C-noise;[f] Cl/C = 0.87	$PtCl_6^{2-} \gg SO_4^{2-}$
0.10 M K_2SO_4[g] 50 μM K_2IrCl_6	S/C-noise;[f] Cl/C = 0.78	$IrCl_6^{2-} \gg SO_4^{2-}$

[a] Signal intensities (peak-to-peak height) are all relative to the C (272 eV) signal and are taken from depth profile analyses like those depicted in Figure 4. Data are from a portion of the depth profile where element ratios are the most constant. [b] Aqueous solution (~25 mL) from which an electrode bearing $(PQ^{2+}\cdot 2Br^-)_n$ (coverage in the range 5×10^{-9} to 5×10^{-8} mol/cm^2) was withdrawn after equilibration for 15 min at 25 °C. [c] Signals given are only those characteristic of the anion. Except where noted, there was no interference in the energy window used in the depth profile. [d] The I signal and 0 signal near 503 eV interfere, but when I^- is present the signal in this energy range is larger. The I^- signal is characteristic because it has two peaks, whereas the 0 signal has only one. [e] These data were recorded using a 3-keV electron beam; all other data were recorded using a 5-keV electron beam. This may cause some variability in the element ratios. [f] No signal beyond background was detectable. [g] These data are from an Auger spectrum without sputtering; cf. Figure 2.

$(PQ^{2+/+\cdot})_n$-coated electrodes. Only when the anion is strongly bound do we observe adverse effects on the kinetics of $(PQ^{2+/+\cdot})_n$ redox system.

Summary

Electrochemical and Auger spectroscopic data establish a wide range of relative binding of anions to surfaces functionalized with $(PQ^{2+})_n$. Large, substitution inert, anionic transition metal complexes such as $IrCl_6^{2-/3-}$, $Fe(CN)_6^{3-/4-}$, $Ru(CN)_6^{3-/4-}$, $Mo(CN)_8^{3-/4-}$, and $Co(CN)_6^{3-}$ have all been found to be tightly bound against anions such as I^-, Br^-, Cl^-, SCN^-, ClO_4^-, SO_4^{2-}, or *p*-toluenesulfonate. The thermodynamically weakly bound anions are labile, rapidly displaced, and do not significantly alter the kinetics for the $(PQ^{2+/+\cdot})_n$ redox system. The strongly bound anions are not kinetically labile and do adversely affect the kinetics for the $(PQ^{2+/+\cdot})_n$ system. The correlation of the relative binding of $IrCl_6^{2-}$ vs. SO_4^{2-} using electrochemical and Auger detection establishes Auger spectroscopy to be a reliable and useful technique to determine the surface elemental composition of electrode surfaces modified with the $(PQ^{2+})_n$ system. The electrochemical data support the conclusion that the capacity of the $(PQ^{2+})_n$-coated electrodes to bind transition metal complexes is determined by the number of PQ^{2+} centers and the charge on the complex. Generally, complex anions can be bound to an extent that reflects complete charge compensation of the polyion bound to the surface. Finally, thermodynamics, not kinetics, has been shown to control the distribution of anions present in the surface bound $(PQ^{2+})_n$ when the electrolyte includes two or more anions.

Acknowledgment. We acknowledge the Office of Naval Research for partial support of this research. Support from the M.I.T. Laboratory for Computer Science, IBM Fund, is also gratefully acknowledged.

Registry No. I, 74173-49-2; *p*-toluene sulfonate, 16722-51-3; $IrCl_6^{2-}$, 16918-91-5; $Fe(CN)_6^{4-}$, 13408-63-4; $Ru(CN)_6^{4-}$, 21029-33-4; $Mo(CN)_8^{4-}$, 17923-49-8; Cl^-, 16887-00-6; $Co(CN)_6^{3-}$, 14897-04-2; I^-, 20461-54-5; SO_4^-, 14808-79-8; Br^-, 24959-67-9; SCN^-, 302-04-5; ClO_4^-, 14797-73-0; $PtCl_6^{2-}$, 16871-54-8.